Selective Patterning of Gold Surfaces by Core-Shell, Semi-Soft Hybrid Nanoparticles

John Moraes,[A,B] Kohji Ohno,[C] Thomas Maschmeyer[D] and Sébastien Perrier[A,E*]

[A] *Key Centre for Polymers & Colloids, School of Chemistry, The University of Sydney, NSW 2006, Australia.*

[B] *Current address: École Polytechnique Fédérale de Lausanne (EPFL), Institut des Matériaux, Laboratoire des Polymères, Bâtiment MXD, Station 12, CH-1015 Lausanne, Switzerland*

[C] *Institute for Chemical Research, Kyoto University, Uji, Kyoto 611-0011, Japan.*

[D] *Laboratory of Advanced Catalysis for Sustainability, School of Chemistry, The University of Sydney, NSW 2006, Australia*

[E] *Current address: Department of Chemistry, University of Warwick, CV4 7AL, UK*

* *s.perrier@warwick.ac.uk, Tel: +44 2476 528085; Fax: +44 25476 524112*

Abstract

We demonstrate the generation of patterned surfaces with well-defined nano- and micro-domains by attaching core-shell, semi-soft nanoparticles of narrow size distribution to micro-domains of a gold-coated silicon wafer. Near monodisperse nanoparticles were prepared by using reversible addition-fragmentation chain transfer (RAFT) polymerization, initiated from a silica surface, to prepare a polystyrene shell around a silica core. The particles were then used as prepared, or after aminolysis of the terminal thiocarbonyl group of the polystyrene shell, to give thiol-terminated nanoparticles. When gold-coated silicon wafers were immersed into very dilute (as low as 0.004 wt. %) suspensions of these particles, both types of particles were shown to adhere to the gold domains. The thiolated particles adhered selectively to the gold micro-domains, allowing for micro-domain patterning, whilst particles that contained the trithiocarbonate functionality led to a much more even coverage of the gold surface with fewer particle aggregations.

Introduction

The concept of micro- or nano-patterning surfaces is an area of research that is attracting growing attention,[1,2] as patterned surfaces show promise for a wide range of exciting applications, such as cell-localisation,[3-5] self-cleaning surfaces,[6,7] atmospheric moisture capture[8] and photonic devices.[9] A typical approach to the manufacture of such surfaces is to deposit nano- or micro-domains of a

polymeric material onto a flat substrate to form a three-dimensional structure. Most such applications require excellent control over the size of, both, nano- and micro-domains, a need that is not well addressed by current manufacturing processes. In addition, the fabrication of three-dimensional patterns, as opposed to monolayer thin-films, often involves intricate sample preparation and several time-consuming steps to obtain a patterned surface.[1,2,10-12] Indeed, most methods for achieving patterns of polymeric materials on substrates, such as micro-contact printing,[13-15] micro-contact moulding,[16] photolithography,[1,5] chemical lithography,[17,18] or using humidified air to form a 'breath-figure' pattern[19] are not scalable in a cost-effective manner, and do not lead to nano- and micro-domains of precise dimensions. Our aim in this work was to develop a system for introducing well-defined nano- and micro-domains on a surface *via* the directed adhesion of nanoparticles. We sought to combine nanoparticles, obtained from reversible addition-fragmentation chain transfer (RAFT) polymerization, with sulfur-bearing functional groups (in particular thiols), which have a well-known affinity for gold,[15,20,21] to achieve these patterned domains.

We have previously demonstrated the versatility of RAFT to graft a polymer shell onto a silica core using a variety of monomers to yield functional core-shell, semi-soft particles of narrow size distribution.[22,23] A fine degree of control over the size of the particles is accessible either *via* the choice of silica core dimensions, or *via* the length of grafted polymer chain. The high density of polymer brushes at the surface of our particles ensures optimal presentation of the free chain-end of the grafted brushes. Furthermore, in polymers obtained from the RAFT process, facile aminolysis of the dithioester at the chain-end yields a thiol,[24] which offers several avenues for post-polymerization modification of polymer chains using highly efficient reactions such as thiol-ene,[25] thiol-yne,[26] or thiol-isocyanate.[27] As a result, this feature has also led several researchers to use RAFT-mediated polymers to modify gold surfaces for a variety of material applications.[28-31] While this technique has been demonstrated with small molecules and polymers, thus far there have been no reports of using RAFT-derived nano- or micro-scopic solid objects to effect the modification of gold surfaces.

Here, we demonstrate the post-polymerization modification of silica-core polystyrene-shell particles, prepared *via* RAFT, into thiolated particles. The thiol groups can not only be easily derivatised with small molecules, but they can also be used to anchor the particles selectively to

gold surfaces, generating a microstructured surface. Surfaces such as these, containing discrete domains of polymer, have several potential applications in fields such as microfluidics[32] and controlling the adhesion and growth of cells.[5] Therefore, the ability to design and access such surfaces *via* robust and scalable techniques, as we demonstrate here, gives researchers a new nano-fabrication tool with which to build structured, functional surfaces.

Results and Discussion

Silica particles with an average diameter of 130 nm were modified with a silane–functionalised RAFT agent as described by Ohno *et al*.[22] to afford RAFT-functionalised particles with a grafting density of 0.4 RAFT groups/nm^2. The applicability of this approach to yield core-shell nanoparticles from a variety of monomeric precursors has previously been demonstrated, however, in the current work we restrict our investigations to silica-polystyrene core-shell particles.[22,23] Silica-supported-RAFT-mediated polymerization of styrene was performed using thermal autoinitiation at 110 °C. On completion of the reaction the particles were 'washed' with several centrifugation-redispersion cycles to remove any physisorbed polymer chains. The successful grafting of polystyrene onto the particles was verified by the increase in particles size from 130 nm to 330 nm by dynamic light scattering (DLS), by the appearance of a polymer shell surrounding each individual particle in transmission electron microscope (TEM) images and by the mass lost on thermolysis as measured by thermogravimetric analysis (TGA, which shows that the hybrid particles contain 44 wt. % of polystyrene). In addition, this approach leads to particles nearly monodisperse in size, with a polydispersity index (*PDI*) of 0.007.

Having obtained the silica-polystyrene hybrid nanoparticles, we proceeded to use isopropylamine to aminolise the terminal RAFT group of the polymer chains to a thiol.[33] After an overnight reaction at room temperature (**Scheme 1**), the particles were collected and washed by successive centrifugation-redispersion cycles with THF. Traditionally, the preferred method to confirm complete removal of the trithiocarbonate functionality is UV-Vis spectrophotometry, which in the case of a successful reaction would show the disappearance of the peak at 308 nm, characteristic of the trithiocarbonate group upon aminolysis.[34] In this case, since the presence of 130 nm silica particles leads to significant scattering of the incident beam, thus rendering direct UV-Vis analysis

of the particles inappropriate, we conducted UV-Vis analysis of the supernatant of the aminolysis reaction.

Scheme 1: Aminolysis of trithiocarbonate from silica-polystyrene hybrid nanoparticles using isopropylamine.

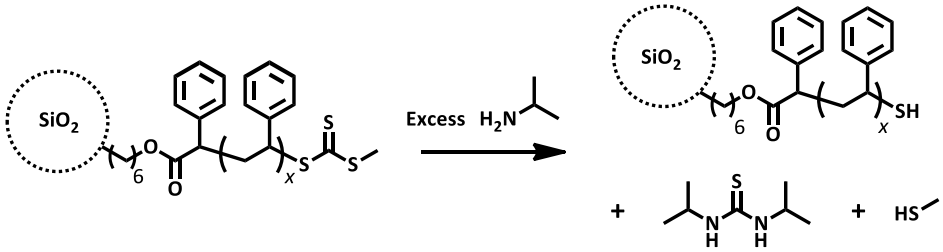

The supernatant solution was separated from the particles by centrifugation. The solvent THF as well as the excess isopropyl amine were removed under reduced pressure. A THF solution of the subsequent residue showed a peak at 250 nm attributable to diisopropylthiourea, a by-product of the aminolysis (dashed line, **Figure 1**). Any methane thiol by-product generated would be removed along with unreacted isopropyl amine *in vaccuo*. The peak at 250 nm is distinct from the characteristic absorption of the trithiocarbonate RAFT agent, PABTC at 308 nm (solid line, **Figure 1**). The particles recovered from this reaction were 'washed' repeatedly with THF and subjected to a second aminolysis under identical conditions as described above. The supernatant of this second aminolysis did not show a peak at 250 nm, but instead one at 277 nm (dotted line, **Figure 1**). This we attribute to polystyrene liberated from the particles by aminolysis, driven by the sterically-unhindered primary amine, of the ester bond that anchors the RAFT agent (and consequently the polymer) to the particle. Indeed, a small shoulder at 277 nm is also visible in the UV-Vis spectrum of the supernatant collected from the first aminolysis, indicating that there is some loss of polystyrene even in the first reaction. However, this is understandable given the large excess (*ca.* 80-fold) of isopropyl amine used. Confirmation that the material is, indeed, a RAFT-grafted polymer was found in SEC analysis of the aminolysis supernatant, which showed that the chains recovered have a molecular weight relatively close to that of the free polystyrene chains recovered from the original polymerization (322 kg/mol polystyrene from aminolysis; 194 kg/mol free polystyrene chains; **ESI Table S1**). The difference in molecular weights of the two species derives from the fact that, compared to the fixed chains, the free chains are influenced to a greater extent by the number of radicals generated *via* thermal autoinitiation.[22] The loss of polystyrene is also evident in the TGA analyses of the samples before and after aminolysis, which show a lowered

organic content on aminolysis (**ESI Figure S1**). Despite this loss of grafted polymer, TEM images of the particles after aminolysis shows them packed in a 2D array that is typical for core-shell particles,[22,23] thus qualitatively demonstrating that the aminolysis does not affect the uniformity of the polymer coating (**ESI Figure S2**). The particles also remained well dispersed in THF although there was significantly greater difficulty in dispersing the aminolysed particles than the particles containing intact RAFT agent. We ascribe this to the presence of surface thiols, which on oxidation into interparticulate disulfide bonds might lead to particle aggregation. Indeed, DLS of the particles indicates that, while a relatively low *PDI* is maintained (0.047), the particles show an apparent increase in size (from 330 nm to 440 nm) consistent with disulfide bridges being present (**ESI Figure S3**).

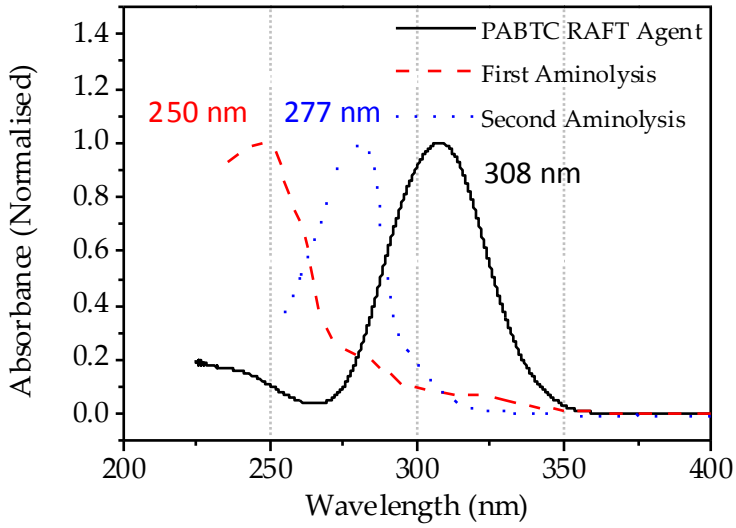

Figure 1: UV-Vis spectra of PABTC, supernatant of first and second aminolysis of silica-polystyrene hybrid nanoparticles in THF.

^{1}H-NMR, TGA and elemental analysis were ineffective at quantifying the success of the aminolysis. Since the trithiocarbonate and corresponding thiol were only minute components of the hybrid nanoparticles (approximately 0.07 wt. % and one trithiocarbonate group per 3,100 repeat units of styrene) and the presence (or lack) of these components could not be detected adequately with these techniques. However, to nonetheless clearly demonstrate the success of the aminolysis, and to establish the accessibility of the particle-bound thiols for chemical reactions, a test reaction was investigated *via* a thio-Michael addition: the particles with the thiol termini were dispersed in THF and added to a vial containing pyren-1-ylmethyl acrylate and dimethylphenyl phosphine (DMPP).

The suspension was then stirred at room temperature for 30 minutes, after which the particles were washed using several centrifugation-redispersion cycles. These cycles were repeated until the supernatant displayed no fluorescence under a 365 nm UV lamp, thereby ensuring that any unbound fluorescent moieties were separated from the particles. The complete removal of pyren-1-ylmethyl acrylate from the supernatant was further confirmed by the lack of aromatic or vinylic signals in the ^{1}H-NMR of the supernatant of the final wash cycle.

The particles, once purified, showed a distinct fluorescence under a 365 nm UV lamp (**Figure 2A**). A control sample was also prepared, *i.e.* a sample of polystyrene-grafted silica particles with the RAFT agent intact was stirred with pyren-1-ylmethyl acrylate for 48 hours and then washed until the supernatant showed no fluorescence. Comparing the thiolated particles (**Figure 2A**) to these particles (**Figure 2B**) under 365 nm of UV light shows a much greater fluorescence intensity in the former, demonstrating that this fluorescence is not simply a result of the pyrenic moieties being entrapped in the polymer chains.

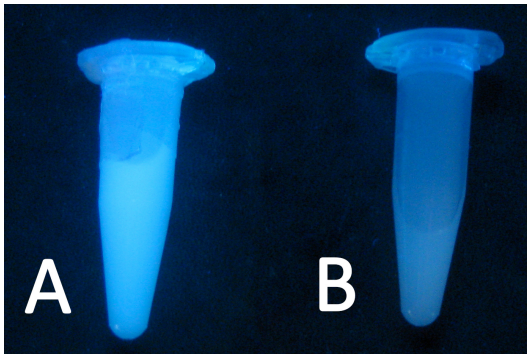

Figure 2: THF suspensions of silica-polystyrene hybrid nanoparticles A) with and B) without chemically bound pyren-1-ylmethyl acrylate under UV light (365 nm).

Having confirmed the reactivity of the nanoparticle-bound thiol groups towards small molecules, we used them to modify gold surfaces. Silicon wafers sputter-coated with gold (an approximately 15 nm layer) were immersed into dilute THF-suspensions of thiolated silica-polystyrene particles and subsequently rinsed with fresh THF. Optical micrographs of the wafers show that discrete domains of material have been deposited regardless of the concentrations of the colloidal suspensions (white arrows, **Figure 3A-C**). We attribute the presence of the large features in the micrographs to aggregates of the particles formed *via* disulfide bonds. The micrographs also show that the size of the aggregates does not depend on concentration in a straightforward manner, *i.e.*

larger aggregates appear on the wafer placed in the 0.004 wt. % suspension than on those on the wafer placed in a 0.04 wt. % suspension. Analogously to nucleation in common crystallisation, higher concentrations lead to many small crystallites and conversely lower concentrations lead to fewer, but larger crystallites. Therefore, we postulate that these larger aggregates, obtained from the lower concentration suspensions, are most likely formed prior to the localisation of the particles on the gold surface. In addition, it is notable that the areas surrounding them appear bereft of particles (black arrows, **Figure 3A-C**). We postulate that this is because the large aggregates when deposited from solution are swollen with THF, which subsequently evaporates as the wafer is dried and causes the aggregate to shrink exposing the underlying wafer. Immersion of a wafer in fresh THF for a further 48 hours did not appear to change the number of aggregates nor particles on the surface (See **Figure 3B and 3D**). Similarly, Soxhlet extraction of the wafer in dichloromethane (a good solvent for the polymer shell) did not dislodge the particles.

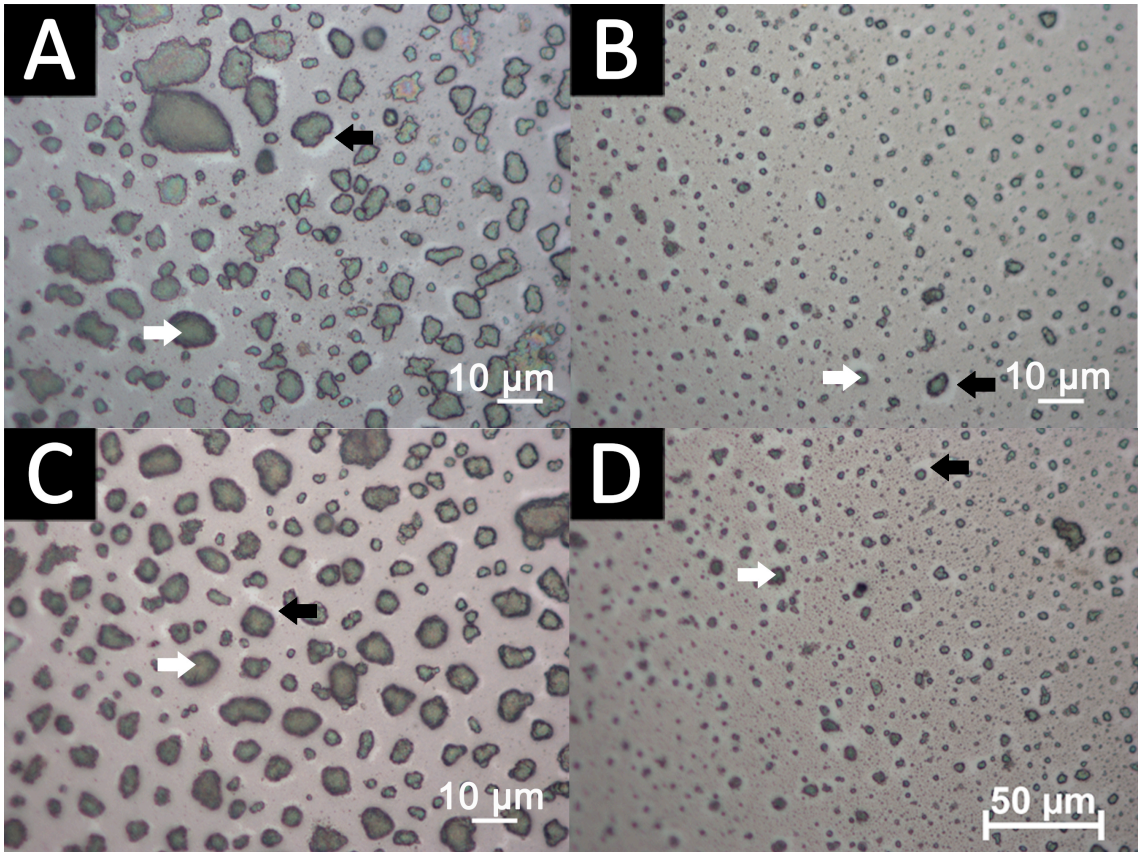

Figure 3: Gold-coated silicon wafers soaked overnight in suspensions of thiolated silica-polystyrene hybrid nanoparticles A) 0.09 wt. %, B) 0.04 wt. %, C) 0.004 wt. % and D) 0.04 wt. % and then soaked for 48 hours in fresh THF. Aggregates are indicated with white arrows and bare areas with black arrows. Scale bars are 10 µm, 10 µm, 10 µm and 50 µm respectively.

Scanning electron microscopy (SEM) images of the areas without aggregates (ESI Figure S4) show that even in these areas, which appear almost featureless in the optical micrographs, approximately 40 % of the gold surface is covered with a monolayer of the silica-polystyrene hybrid nanoparticles (**ESI Figure S4**). We attribute the lack of total surface coverage to two factors: 1) a single particle bound to the wafer will present significant steric hindrance to another particle to bind in close proximity and 2) the particles adhere to the gold surface, while the polymer chain is swollen with a good solvent (THF) that upon evaporation causes the chains to shrink and leaves discrete particles (an identical effect to what was observed with the large aggregates). Indeed, we calculate that even at the lowest concentrations used, there are at least ten times as many particles in suspension than are required for a complete coverage of the wafer surface and the absence of a pervasive monolayer is due to the two factors above. The fact that the particles remain strongly bound onto the silicon wafer even after the rinsing steps suggests that they are not merely physically adsorbed onto the gold surface. The vast majority of the nanoparticles appear alone or in clusters of two or three particles. In addition, there are several, larger clusters of particles. The presence of these larger aggregates cause the dark features on the optical micrograph in **Figure 3**. However, the attempts to disrupt the larger clusters of nanoparticles prior to deposition on the gold plate by filtering and sonication of the suspension were unsuccessful. As per above, we hypothesise that these clusters formed in the supernatant independent of wafer immersion. Since the aggregates are likely due to disulfide bridges between particles, we also tested particles containing the unmodified trithiocarbonate chain-end-group that remained from the RAFT process. A wafer was immersed into a THF suspension (0.05 wt. %) of polystyrene-grafted silica particles and then subsequently rinsed with fresh THF, as in the previous experiments. The optical micrograph (**Figure 4**) of such a gold-coated wafer showed that there were far fewer of the large aggregations of particles than were present in the corresponding experiment with thiolated particles (**Figure 3B**). This observation is borne out by the SEM image of the wafer (**Figure 4B**), which shows very few aggregations of greater than three particles when compared to the corresponding SEM image with thiolated particles (**ESI Figure S4**). The particles in this case occur in evenly-spaced arrangements reminiscent of the arrays of gold nanodots reported by Spatz *et al.*, albeit on a larger scale.[35,36] It is significant that the particles are deposited onto the gold surface from solution rather than by dip-coating. The trithiocarbonate group anchors the particles to the gold surface,[28,37] while the polymer chain swollen with THF spaces the particles at uniform

intervals. On removal of the solvent, the polymer chain shrinks leaving the particles discretely spaced as seen in **Figure 4B**. The ability of the trithiocarbonate to bind to gold is thus highly significant, as it eliminates the aminolysis step from the series of reactions required to functionalise gold surfaces with the hybrid nanoparticles. The fact that the particles do not aggregate means that a much more even coating of the gold surface can be obtained. This is a very promising method to easily achieve a three-dimensional, robust micro-pattern on a flat substrate.

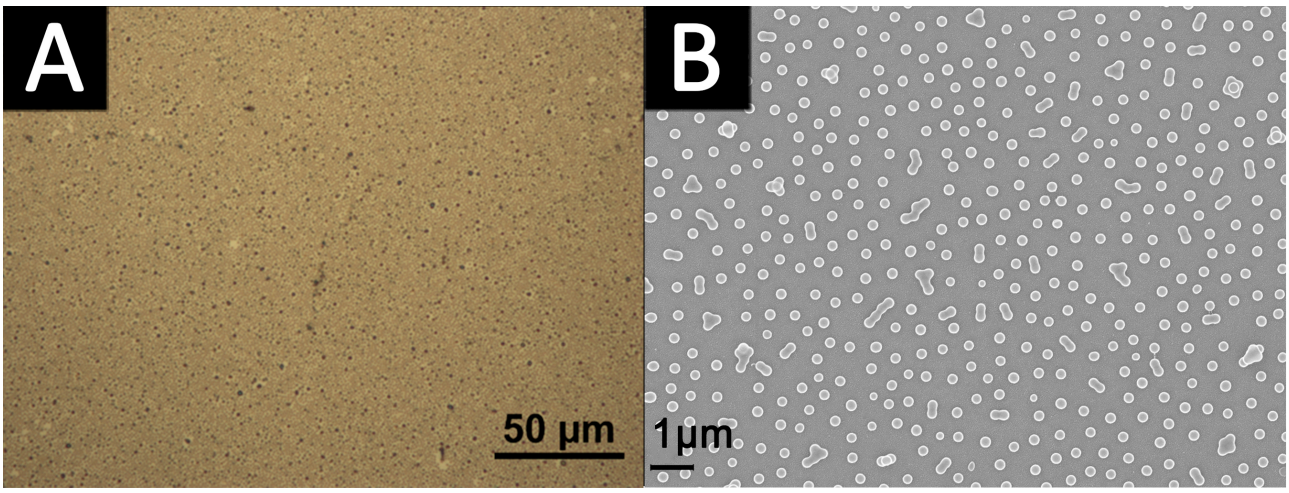

Figure 4: A) Optical image and B) SEM image of a gold-coated silicon wafer immersed in a suspension of Si-pS-RAFT (0.05 wt. %). Scale bars are 50 µm and 1 µm respectively.

In order to demonstrate the selectivity of the particles for gold, a silicon surface was patterned with gold so that there were distinct gold and silicon domains (as confirmed with SEM and EDX images that demonstrate the fidelity of the pattern transfer over a several square millimetre area, **ESI Figure S5**). Wafers, thus patterned, were immersed into suspension of silica-polystyrene hybrid particles with both trithiocarbonate and thiol functionalities at their surfaces. After allowing the plates to stand overnight without agitation, they were subsequently rinsed, dried and imaged. Distinct results were obtained depending on the functionality at the particle termini: particles with the trithiocarbonate intact were observed throughout the surface demonstrating non-specificity to the gold micro-domains (**ESI Figure S6**). The binding ability to gold of trithiocarbonates,[28,37] as well as xanthates,[38] has been reported before, and it is therefore unsurprising to observe a strong affinity of the particles to the gold surface. It is however remarkable to observe a similar attachment of the particles to the silicon substrate. The litterature provides many examples of adsorption of thionocarbamates onto various surfaces, in particular oxidised surfaces.[39] We therefore hypothesise that the trithiocarbonate group adsorbs strongly to the natively-oxidised

silicon, which results in the deposition of particles on the silicon domains. In contrast, the wafer immersed in the suspension of silica-polystyrene particles with thiol functionality shows that the particles have been selectively deposited only in the regions containing gold (**Figure 5A-C**). The darker grid of uncoated silicon is bereft of particles. This selectivity is evident over the entire wafer (**Figure 5**) and is preserved with high fidelity (**Figure 5B-C**) on most of the boundaries of the two domains.

Atomic force microscopy (AFM) of the boundary between the gold and silicon (**Figure 5D**) demonstrates that the height of the larger clusters is indeed as would be expected for aggregations of hybrid nanoparticles. While few aggregates are noted, the vast majority of the particles appear to be bound directly to the gold surface. **Figure 5D** also shows that while the demarcation between silicon and gold is made clearly visible by the number of particles present or each surface, there are still a few stray particles on the silicon domain. The interaction between the particles and silicon is clearly not as favourable as the thiol-gold interaction as evidenced by the clear preference of the particles for the gold domain. Despite these few particles on the silicon regions, however, the almost totally selective deposition of the hybrid nanoparticles on the areas of gold has been clearly demonstrated. The selective deposition was achieved in two steps, *i.e.* that of patterning the surface and the deposition of particles. The first step was shown to be readily achievable over several square millimetres of area but in principle may scaled to any size as long as a gold coating is present. While the second step does indeed use an overnight immersion, it proceeds readily at room temperature from a dilute suspension of particles and thus is also a scalable process. This is a, thus, a very promising method for functionalising surfaces with polymeric nano-domains which have shown to be extremely useful in controlling hydrophobicity[40,41] and cell adhesion.[42]

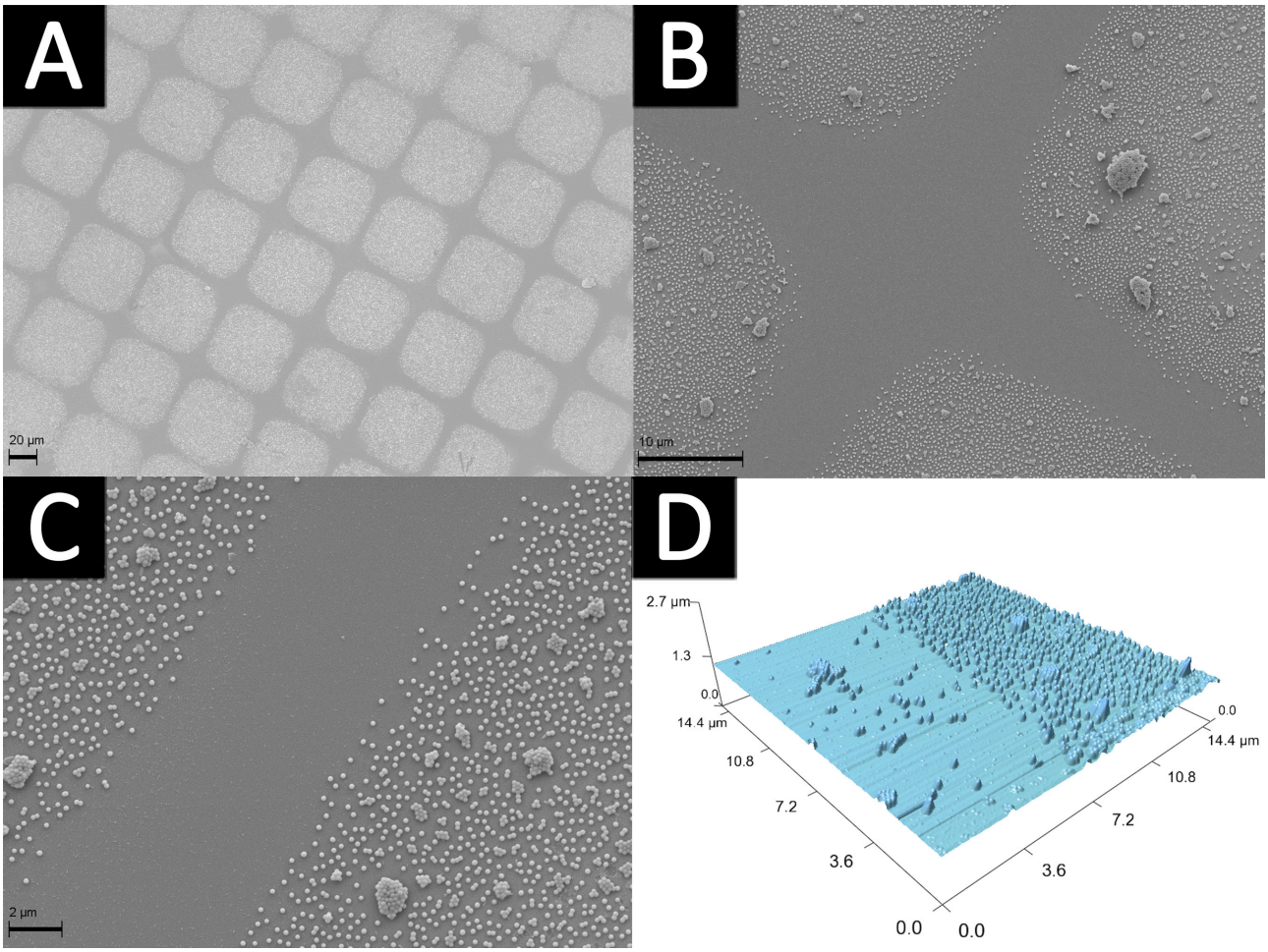

Figure 5: A-C) SEM images and D) AFM image of a patterned silicon wafer upon immersion in a 0.004 wt. % suspension of thiolated silica-polystyrene particles. Scale bars for images A, B and C are 20 µm, 10 µm, and 2 µm respectively.

Summary

We have demonstrated a simple two-step procedure for the design of patterned surfaces with well-defined nano- and micro-domains by coating gold surfaces with near monodisperse silica-polymer hybrid nanoparticles, functionalised with either thiols or trithiocarbonates. The method can be used to deposit particles from very dilute suspensions, so that discrete domains of polymer can be located on the gold surface. The very narrow size distribution of the particles provides well-defined nano-domains, whilst the gold patterning leads to micro-domains of precise dimensions. While the greatest selectivity for gold has been demonstrated when particles with thiolated functionalities are used, allowing for micro-domain templating, particles that exhibit a trithiocarbonate functionality have also been shown to adhere to gold, and lead to much more even coverage of the gold surface with fewer particle aggregations allowing for nano-domain

templating. These surfaces showing patterning at the micro- and nano-scale have several potential applications in fields such as microfluidics[32] and controlling the adhesion and growth of cells.[5]

Experimental

Materials

Reagents were purchased from Sigma-Aldrich at the highest purity and used as received unless otherwise stated. Styrene was passed through a column of activated neutral alumina in order to remove the inhibitor before use. Silica particles (SEAHOSTER KE-E10, average diameter = 130 nm, 20 wt. % suspension in ethylene glycol) were kindly donated by Nippon Shokubai Co., Ltd., Osaka, Japan. 2-(Butylthiocarbonothioylthio)propionic acid (PABTC) was kindly provided by Algi Serelis of Dulux Group Australia. Polymerizations were carried out under a N_2 atmosphere. Pyren-1-ylmethyl acrylate was synthesised by the reaction of 1-pyrenemethanol and acryloyl chloride as previously reported.[43]

Equipment

Molar mass distributions were measured using SEC on a Shimadzu LC-10AT liquid chromatograph system with a Polymer Laboratories PLgel 5 μM guard column and two PLgel Mixed-B columns using THF at 1.0 mL/min as the eluent at 40 °C. The system was equipped with a Shimadzu RID-10A differential refractive index detector and a Shimadzu SPD-10A UV-Vis detector. Polystyrene standards were used to calibrate the SEC system. Analyte samples contained 0.5 vol % toluene as the flow rate marker. ^{1}H-NMR spectra were acquired on a Bruker 300 MHz in deuterated chloroform. All chemical shifts are reported in ppm (δ). UV-Vis spectra were collected on a Cary 4E UV spectrophotometer running Cary Scan software.

Dynamic Light Scattering (DLS) was conducted on a Malvern High Performance Particle Sizer running Dispersion Technology Software (Version 4.00). Thermogravimetric analysis (TGA) was conducted on a TA Instruments Hi-res TGA 2950 instrument using Thermal Advantage v1.1A software. The instrument was continuously purged with N_2 gas. Samples were heated to 100 °C and equilibrated at that temperature to remove residual water prior to analysis. Data was analysed using TA Instruments' Universal Analysis 2000 software v4.2E.

Transmission electron microscope (TEM) images were obtained on a JEOL 1400 120kV TEM with a LaB_6 filament running Gatan Digital Micrograph software. SEM images were obtained on a Zeiss ULTRA *plus* scanning electron microscope. Samples on silicon wafers were mounted on aluminium stubs with carbon tape. Samples on TEM grids were imaged using an aluminium holder without further treatment. Optical images were obtained under a reflection optical microscope (Nikon Instruments LV-150) using Nikon NIS Elements software. Topography AFM images were obtained by tapping mode in air (Asylum Research, MFP-3D-SA) with the assistance of Dr Andrew Telford.

Silica-supported RAFT-mediated polymerization of styrene

In a typical reaction, to 14.43 g (138.6 mmol) of deinhibited styrene was added 8.2 mg (34 μmol) of PABTC, 576.5 mg (3.768 mmol) of DMF and 1.402 g of a 13.34 wt. % suspension of the RAFT-functionalised silica particles in DMF. This suspension was agitated to ensure perfect dispersion of the particles and transferred into glass vials equipped with a magnetic stirring flea and rubber septum. The vial was deoxygenated by purging it with nitrogen for 20 minutes before immersing it into an oil-bath thermostatted at 110 °C to begin RAFT polymerization. After 16.5 hours, the vial was removed from the oil-bath, cooled to room temperature and opened to atmosphere to introduce oxygen and quench the polymerization. An aliquot was taken and dissolved in deuterated chloroform for ^{1}H-NMR analysis. The remainder of each reaction mixture was diluted with THF and washed with three centrifugation-redispersion cycles in (3 x 25 mL) THF to recover the silica-polystyrene hybrid nanoparticles of size 330 nm and polydispersity 0.007, according to DLS.

Aminolysis of silica-polystyrene hybrid nanoparticles

To 4.00 g of a suspension of silica-polystyrene hybrid nanoparticles (0.87 wt. % in THF, *ca.* 7.8 μmol of RAFT agent) was added isopropyl amine (37.5 mg, 634 μmol) and THF (1.04 g, 14.5 mmol). The resulting suspension was placed in a glass vial with a magnetic stirrer flea and sealed with a rubber septum. The suspension was purged with nitrogen whilst in an ice-bath and then stirred overnight at room temperature. The particles were collected by centrifugation and washed in THF by successive centrifugation-redispersion cycles before being redispersed in THF for DLS, UV-Vis, TEM and SEM analysis. Samples were dried in a vacuum oven before TGA and elemental analysis.

The solvent from the supernatant was removed by rotary evaporation before the residues were dissolved in THF for UV-Vis analysis or $CDCl_3$ for ^{1}H-NMR analyses. The particle suspension in THF was found to have an average size of 440 nm and a *PDI* of 0.047 by DLS.

Addition of pyren-1-ylmethyl acrylate to silica-polystyrene hybrid nanoparticles

Following a similar procedure as that described by Chan *et al.*,[44] 940 mg of a 3.21 wt. % suspension of silica-polystyrene hybrid nanoparticles in THF was added to a solution containing 0.6 mg (2 μmol) of pyren-1-ylmethyl acrylate and 36 mg (26 μmol) of dimethylphenyl phosphine (DMPP) in 368 mg (17.7 mmol in total) THF.[43] The suspension was then agitated at room temperature for 30 minutes before the particles were washed by centrifugation and redispersion cycles in THF to remove unreacted DMPP and pyren-1-ylmethyl acrylate before drying the particles for TGA analysis.

General procedure for sputter-coating gold onto silicon

Silicon wafers were cleaned by exposing them to air plasma for 30 s (Harrick Plasma, Ithaca NY, model PDC-002). The wafers were then sputter-coated with gold (Emitech K550X sputter coater) using a 25 mA current and a 2 minute deposition time to achieve a gold coating of *ca.* 15 nm. In order to obtain a patterned surface, a copper grid was first placed on a freshly-cleaned silicon wafer and immobilized with tape. The wafer was then sputter-coated with gold as described above and the tape and grid were removed. The wafer was then immersed in THF to remove any residue left by the tape, dried and then cleaned with plasma immediately prior to immersion in suspensions of the hybrid nanoparticles.

General procedure for depositing particles on surfaces

Gold-coated silicon wafers were immersed into suspensions of silica-polymer hybrid nanoparticles in THF. The THF suspensions of particles were contained in glass vials sealed with plastic screw-caps to prevent evaporation of the solvent. The vials were allowed to stand overnight at room temperature without agitation. The wafers were then washed by placing them in fresh THF contained in glass vials with plastic screw-caps and agitating them by swirling the vials. The wafers were then allowed to stand in the glass vials for ten minutes. This was done twice before

the wafers were dried by blowing a gentle stream of nitrogen over them. The wafers were then imaged either optically or *via* SEM without further coating.

Acknowledgements

The authors thank Dr. Andrew Telford and Dr. Chiara Neto for obtaining the AFM measurements. Funding from the Australian Research Council's Discovery, Future Fellowship and Linkage Programs is acknowledged by S.P. and T.M. J.M. acknowledges the Henry Bertie & Florence Mabel Gritton Scholarship, The O'Donnell Young Scientist Prize and CSIRO PhD studentship. The authors acknowledge the facilities, and the scientific and technical assistance, of the Australian Microscopy & Microanalysis Research Facility at the University of Sydney.

References

(1) Nie, Z. H.; Kumacheva, E. *Nat. Mater.* **2008**, *7*, 277.

(2) Lei, Y.; Yang, S.; Wu, M.; Wilde, G. *Chem. Soc. Rev.* **2011**, *40*, 1247.

(3) Telford, A. M.; Meagher, L.; Glattauer, V.; Gengenbach, T. R.; Easton, C. D.; Neto, C. *Biomacromolecules* **2012**, *13* 2989.

(4) Kaji, H.; Camci-Unal, G.; Langer, R.; Khademhosseini, A. *Biochim. Biophys. Acta* **2011**, *1810*, 239.

(5) Ogaki, R.; Alexander, M.; Kingshott, P. *Mater. Today* **2010**, *13*, 22.

(6) Park, K. C.; Choi, H. J.; Chang, C. H.; Cohen, R. E.; McKinley, G. H.; Barbastathis, G. *ACS Nano* **2012**, *6*, 3789.

(7) Blossey, R. *Nat. Mater.* **2003**, *2*, 301.

(8) Thickett, S. C.; Neto, C.; Harris, A. T. *Adv. Mater.* **2011**, *23*, 3718.

(9) Scofield, A. C.; Kim, S.-H.; Shapiro, J. N.; Lin, A.; Liang, B.; Scherer, A.; Huffaker, D. L. *Nano Lett.* **2011**, *11*, 5387.

(10) Demers, L. M.; Mirkin, C. A. *Angew. Chem., Int. Ed.* **2001**, *40*, 3069.

(11) Tanaka, M.; Hosaka, T.; Tanii, T.; Ohdomari, I.; Nishide, H. *Chem. Commun.* **2004**, 978.

(12) Shiu, J. Y.; Kuo, C. W.; Chen, P. L.; Mou, C. Y. *Chem. Mater.* **2004**, *16*, 561.

(13) Bracher, P. J.; Gupta, M.; Whitesides, G. M. *J. Mater. Chem.* **2010**, *20*, 5117.

(14) Shah, R. R.; Merreceyes, D.; Husemann, M.; Rees, I.; Abbott, N. L.; Hawker, C. J.; Hedrick, J. L. *Macromolecules* **2000**, *33*, 597.

(15) Kumar, A.; Whitesides, G. M. *Appl. Phys. Lett.* **1993**, *63*, 2002.

(16) Jhaveri, S. B.; Beinhoff, M.; Hawker, C. J.; Carter, K. R.; Sogah, D. Y. *ACS Nano* **2008**, *2*, 719.

(17) He, Q.; Kuller, A.; Grunze, M.; Li, J. B. *Langmuir* **2007**, *23*, 3981.

(18) He, Q.; Kueller, A.; Schilp, S.; Leisten, F.; Kolb, H. A.; Grunze, M.; Li, J. B. *Small* **2007**, *3*, 1860.

(19) Widawski, G.; Rawiso, M.; Francois, B. *Nature* **1994**, *369*, 387.

(20) Hakkinen, H. *Nature Chem.* **2012**, *4*, 443.

(21) Porter, M. D.; Bright, T. B.; Allara, D. L.; Chidsey, C. E. D. *J. Am. Chem. Soc.* **1987**, *109*, 3559.

(22) Ohno, K.; Ma, Y.; Huang, Y.; Mori, C.; Yahata, Y.; Tsujii, Y.; Maschmeyer, T.; Moraes, J.; Perrier, S. *Macromolecules* **2011**, *44*, 8944.

(23) Moraes, J.; Ohno, K.; Gody, G.; Maschmeyer, T.; Perrier, S. *Beilstein J. Org. Chem.* **2013**, *9*, 1226.

(24) Lima, V.; Jiang, X. L.; Brokken-Zijp, J.; Schoenmakers, P. J.; Klumperman, B.; Van Der Linde, R. *J. Polym. Sci., Part A: Polym. Chem.* **2005**, *43*, 959.

(25) Lowe, A. B. *Polym. Chem.* **2010**, *1*, 17.

(26) Lowe, A. B.; Hoyle, C. E.; Bowman, C. N. *J. Mater. Chem.* **2010**, *20*, 4745.

(27) Li, H.; Yu, B.; Matsushima, H.; Hoyle, C. E.; Lowe, A. B. *Macromolecules* **2009**, *42*, 6537.

(28) Hotchkiss, J. W.; Lowe, A. B.; Boyes, S. G. *Chem. Mater.* **2006**, *19*, 6.

(29) Boyer, C.; Whittaker, M. R.; Nouvel, C.; Davis, T. P. *Macromolecules* **2010**, *43*, 1792.

(30) Lowe, A. B.; Sumerlin, B. S.; Donovan, M. S.; McCormick, C. L. *J. Am. Chem. Soc.* **2002**, *124*, 11562.

(31) Sumerlin, B. S.; Lowe, A. B.; Stroud, P. A.; Zhang, P.; Urban, M. W.; McCormick, C. L. *Langmuir* **2003**, *19*, 5559.

(32) Mijatovic, D.; Eijkel, J. C. T.; van den Berg, A. *Lab Chip* **2005**, *5*, 492.

(33) Qiu, X.-P.; Winnik, F. M. *Macromol. Rapid Commun.* **2006**, *27*, 1648.

(34) Boyer, C.; Granville, A.; Davis, T. P.; Bulmus, V. *J. Polym. Sci., Part A: Polym. Chem.* **2009**, *47*, 3773.

(35) Spatz, J. P.; Mössmer, S.; Hartmann, C.; Möller, M.; Herzog, T.; Krieger, M.; Boyen, H.-G.; Ziemann, P.; Kabius, B. *Langmuir* **1999**, *16*, 407.

(36) Lohmueller, T.; Bock, E.; Spatz, J. P. *Adv. Mater.* **2008**, *20*, 2297.

(37) Duwez, A.-S.; Guillet, P.; Colard, C.; Gohy, J.-F.; Fustin, C.-A. *Macromolecules* **2006**, *39*, 2729.

(38) Ihs, A.; Uvdal, K.; Liedberg, B. *Langmuir* **1993**, *9*, 733.

(39) Mielczarski, J. A.; Yoon, R. H. *Langmuir* **1991**, *7*, 101.

(40) Burton, Z.; Bhushan, B. *Nano Lett.* **2005**, *5*, 1607.

(41) Feng, L.; Li, S.; Li, Y.; Li, H.; Zhang, L.; Zhai, J.; Song, Y.; Liu, B.; Jiang, L.; Zhu, D. *Adv. Mater.* **2002**, *14*, 1857.

(42) Kleinfeld, D.; Kahler, K. H.; Hockberger, P. E. *J. Neurosci.* **1988**, *8*, 4098.

(43) Moraes, J.; Ohno, K.; Maschmeyer, T.; Perrier, S. *Chem. Mater.* **2013**.

(44) Chan, J. W.; Hoyle, C. E.; Lowe, A. B. *J. Am. Chem. Soc.* **2009**, *131*, 5751.